Research Square

Preprints are preliminary reports that have not undergone peer review.
They should not be considered conclusive, used to inform clinical practice,
or referenced by the media as validated information.

Biodegradation of malachite green by Pleurotus eryngii: A study on decolorization, mechanism, toxicity, and enzyme

Guoying Lv

lvgy9190163.com

Zhejiang Academy of Agricultural Sciences https://orcid.org/0000-0002-9532-4838

Zuofa Zhang

Zhejiang Academy of Agricultural Sciences

Yingyue Shen

Zhejiang Academy of Agricultural Sciences

Mei Wang

Zhejiang Academy of Agricultural Sciences

Research Article

Keywords: Malachite green, Degradation, Pleurotus eryngii, Mechanism, Toxicity, DyP-type peroxidase

Posted Date: July 6th, 2023

DOI: https://doi.org/10.21203/rs.3.rs-3067023/v1

License: This work is licensed under a Creative Commons Attribution 4.0 International License.
Read Full License

Version of Record: A version of this preprint was published at Environmental Science and Pollution Research on February 19th, 2024. See the published version at https://doi.org/10.1007/s11356-024-32465-0.

Abstract

The purpose of this study was to investigate the biodegradation capability of *Pleurotus eryngii* through decolorizing malachite green (MG), explore the possible mechanism, and test the toxicity. The results indicated that this strain possessed a high decolorizing ability. The intermediates of MG degradation identified by UPLC-TOF-Triple-MS analysis included 4-(dimethylamino)benzophenone, 4-(methylamino)benzophenone, and 4-(dimethylamino)phenol. Moreover, toxicity testing on the zebrafish animal model demonstrated a significant reduction in the toxicity of the degradation products. A newly discovered dye-decolorizing peroxidase (DyP-PE) from *P. eryngii* was amplified, cloned, and expressed. A 56.4 kDa protein of DyP-PE was purified, and this enzyme exhibited good decolorizing properties of MG. Therefore, this strain could potentially be used for the bioremediation of MG pollution, and the DyP-PE in *P. eryngii* may contribute to the degradation of MG.

1. Introduction

Malachite green (MG) is an N-methylated diaminotriarylmethane dye widely used in the textile industry (Zhou et al., 2015). In aquaculture, it is also used as a fungicide and parasiticide (Arumugam et al., 2019). However, MG is highly toxic and can induce carcinogenesis and teratogenicity in human beings (Gopinathan et al., 2015). Once absorbed by fish, MG accumulates in fish tissues (Srivastav and Roy, 2018). Multiple nations have banned MG because it will create significant contamination if it remains in the aquatic environment (Andersen et al., 2018). Due to its low cost and a lack of suitable alternatives, MG is still illegally used in some areas. Furthermore, MG is difficult to decompose naturally because of its complex aromatic molecular structure (Liu et al., 2020). Hence, it is of the utmost importance to find effective and eco-friendly ways to deal with MG pollution.

Several physicochemical methods are available to remove MG pollution, including adsorption (You et al., 2022), photodegradation (Rakhshaee and Darvazeh, 2018), and oxidation (Mohammed Al-Balawi et al., 2023). However, these methods can produce the secondary pollutants. In recent years, researchers have adopted several combined approaches, such as biochar adsorption (Giri et al., 2022) and the immobilization of enzymes (Pandey et al., 2022). Biodegradation using microorganisms has emerged as a promising efficient and environment-friendly alternative. The removal of MG by live microbial cells involves biosorption and biodegradation. MG can be degraded by bacteria, actinobacteria and fungi (Jeon and Lim, 2017; Ting et al. 2021; Adenan et al., 2022; Chaieb et al., 2022). The majority of microorganisms can produce a variety of extracellular enzymes. Numerous papers have demonstrated the role of enzymes in the biodegradation of MG, such as laccase, manganese peroxidase, cytochrome P450 oxygenase, and triphenylmethane reductase. Although microbial systems for dye degradation have been described, it is necessary to evaluate the potential of microbes for dye degradation. Furthermore, understanding the metabolic process is critical for better understanding of the MG biodegradation mechanism.

Pleurotus eryngii, a white-rot fungus, has been intensively investigated for its capacity to degrade and transform benzo [a] pyrene and lignin (Hadibarata et al., 2022). The utilization of biodegradation for the elimination of dyes, particularly MG, is unknown; therefore, the characterisation of microorganisms and investigations on MG utilisation are extremely intriguing. The present study investigated the decolorization and degradation of MG by *P. eryngii*. Different parameters influencing MG degradation were examined. The metabolites involved during biodegradation were also identified and characterized by UPLC-Triple-TOF-MS. The toxicity of MG before and after degradation was also examined. Additionally, DyP-type peroxidase, an important enzyme involved in dye degradation from *P. eryngii*, was cloned, expressed, and characterized. This purpose of this study is to better understand *P. eryngii*s capability for biodegrading MG and provide the framework for future research in the organism's capacity for bioremediation.

2. Materials and methods

2.1 Fungi and reagents

The fungal strain *P. eryngii* was obtained from the China General Microbiological Culture Collection Center (CGMCC5.732) and grown in CYM medium (10 g/L maltose, 20 g/L glucose, 2 g/L yeast extract, 2 g/L peptone, 0.5 g/L $MgSO_4 \cdot 7H_2O$ and 0.5 g/L K_2HPO_4) at 25°C on a rotary shaker at 150 r/min. MG (Purity: >95%) was purchased from Shanghai Baoman Bio-Technology Co., Ltd., China. Other chemicals and organic solvents were analytical reagent grade.

2.2 Decolorization experiments

After the fermentation of *P. eryngii* for 7 days, the mycelia were collected through centrifugation (10, 000 g, 5 min) and then washed with distilled water for three times. The mycelia were suspended in distilled water containing MG to achieve a mycelium concentration of 10.0 g/L (wet weight). The decolorizing tests were conducted under the following conditions: 25°C, pH 7.0, and 50 r/min. To explore the effects on MG decolorization, different initial MG concentrations (10–150 mg/L), temperatures (20–50°C) and initial pH values (4.0–9.0) were investigated. The decolorization was estimated after 120 min of incubation. As a control, a heat-killed mycelia suspension was used. The mixtures were then centrifuged (10, 000 g, 10 min). Then, the absorbance of the supernatant was determined at 617 nm.

The decolorization rate was calculated using the following formula:

Decolorization rate (%) = $(C_0 - C)/C_0 \times 100$,

where C_0 and C are the initial and final concentrations of MG, respectively.

2.3 MG degradation products analysis

UPLC-Tripe-TOF-MS was used to detect the intermediates of MG degradation. To obtain samples, MG or its metabolites were dried and dissolved in a 70% methanol aqueous solution, and then being filtered

through a 0.45 μm membrane. A 10 μL sample was injected into C_{18} (ZORBAX SB C_{18} 100 ×4.6 mm, Agilent, USA). The eluents were conducted as follows: A, 0.1% formic acid and 10 mM ammonium formate in water; B, 0.1% formic acid in acetonitrile. The elution conditions were as follows: 0–5 min, 90% A isocratic; 5–20 min, linear gradient from 90 to 50%; 20–35 min, linear gradient from 50 to 5% A; 35–37 min, 5% A isocratic. The MS conditions were conducted according to the method described in our previous reports (Zhang et al., 2021).

2.4 Toxicity test

Zebrafish embryos were used to evaluate the toxicity of MG and its degradation products. A circulating aquarium system was used to rear the zebrafish (14 h light/10 h dark, 28± 0.5°C). All treatments were conducted according to the regulations of the Institutional Animal Care and Use Committee of Zhejiang University. To select suitable MG concentrations, the embryos were randomly distributed into 1000 mL glass beakers containing 500 mL MG exposure solution (0, 1, 5, 20, 40, 100, and 200 μg/L). Each concentration included six replicates. Zebrafish embryos were exposed to MG solution for 96 h, the heart rate, death rate, and malformation rate of larvae with different MG exposure solutions were counted.

Zebrafish larvae were anesthetized and photographed using a Leica M205 FA stereo microscope (Germany). The liver and yolk sac areas were measured using Image J software. Liver degeneration percentage, liver size change and yolk sac retention were calculated based on the following formulas:

Liver size (% of control) = liver area (MG or its degraded products group)/liver area (control group) ×100%

Yolk sac retention (% of control) = Yolk sac (MG or its degraded products group)/ Yolk sac (control group) ×100%

Liver transparency (%) = [1–liver optical density (MG or its degraded products group)/liver optical density (control group)] ×100%

After administration, zebrafish larvae were fixed, embedded and stained with haematoxylin-eosin (H&E) and observed the histopathological changes in the liver.

2.5 Research on the DyP in *P. eryngii*

The sequence of DyP-type peroxidase was obtained from the JGI website (https://genome.jgi.doe.gov/portal/). The DyP encoding gene (geneID1429886) was amplified from the full-length cDNA of *P. eryngii* using the following primers: forward 5'-CATCATCATCATCATCATATGATGACTACACCTGCACCACC-3' and reverse 5'-CTTGAATTCGGATCCCTCGAGAGCAGAGATTGGAGCTTGGG-3'. The recombinant plasmid pCZN1-PE was obtained by connecting the target segments to the pCZN1 vector using homologous recombination and restriction digestion. The ligated pCZN1-PE plasmid was transferred into *E. coli* Rosetta expression cells. Plasmids were extracted from a single clone, and NdeI-XhoI restriction enzyme was used to digest plasmids to confirm the purpose strip. The recombinant plasmids were sequenced and analyzed using the GenBank BLASTn program (http://www.ncbi.nlm.nih.gov/).

IPTG (Isopropyl β-D-1-thiogalactopyranoside,0.2 mM, 37°C, 4 h) was used to induce the fusion protein. The cells were harvested by centrifugation and disrupted by an ultrasonic homogenizer (Sartorius Labsonic M) to release intracellular proteins followed by centrifugation (12, 000 g, 15 min) to obtain cell-free supernatant. The expression of the target protein was expressed as inclusion bodies in cells by SDS-PAGE analysis. Ion exchange column chromatography was used to purify DyP-PE protein; the column was preequilibrated with binding buffer (20 mM imidazole) and then eluted with elution buffer (500 mM imidazole) to collect protein. A active fraction was collected and analyzed by SDS-PAGE.

To test and verify the ability of the purified DyP-PE to decolorize MG, different concentrations (10, 20, 30, 40, 50, 100 and 150 mg/L) of MG were prepared. The mixture of MG solution (1 mL) and enzyme solution (1 mL, pH 7.0, protein concentration 0.05 mg/mL) was incubated at 30°C for 2 h. The absorbance was monitored at 617 nm.

2.6 Statistical analysis

All data are expressed as the mean value ± standard deviation. Multiple groups were compared using a one-way analysis of variance followed by a *t-test*.

3. Results and discussion

3.1 Parameter optimization for decolorization of MG

The relationship between MG concentration and the rate of decolorization with time was determined by varying the dye concentration ranging from 10 to 150 mg/L and the time ranging from 30 min to 180 min at pH 7 and incubated at 25°C. It was found that the decolorization rate decreases with an increase in MG concentration and rises with increasing time. When the MG concentration increased from 10 to 150 mg/L, the decolorization rates decreased from 47.2–2.32% after 30 min (Fig. 1a) and remained steady after 3 h. Especially at low MG concentrations, the decolorization initial velocity increases as the dye concentration increases. Hence, when the initial MG concentration increased from 10 to 50 mg/L, the MG degradation initial velocity increased from 0.47 to 0.64 mg-MG/g-cell/h, but decreased at higher MG concentrations (100 and 150 mg/L). This result does not conform to the Lineweaver–Burk equation. A higher concentration of MG might have a toxic effect on mycelium. The percentage of degradation decreased as the increasing of MG concentration increased, and similar results were reported by Vignesh et al. (2020). Daneshvar et al. (2007) earlier recorded different MG decolorization trends. Herein, the relationship between the dye concentration and the decolorization efficiency is not changeless; instead, the different microorganisms seem to have a significant influence on decolorization.

The effect of temperature on the decolorization of MG was assessed between 25°C and 55°C to determine an optimum value after 120 min incubation (Fig. 1b). The pH value and dye concentration were kept constant at 7.0 and 20 mg/L, respectively. Initially, the rate of decolorization increased with increasing temperature (20–30°C) and remained steady between 30°C and 50°C. When the temperature

was over 50°C, the decolorization rate decreased evidently. This result indicats that *P. eryngii* is a suitable candidate for the bioremediation of MG at a wide range of temperatures.

To investigate the decolorization behaviors at different initial pH level, batch studies were conducted in the decolorization system with and without mycelia after 120 min incubation (The temperature and MG concentration were both kept constant at 30°C and 20 mg/L, respectively). The experiments indicated that no obvious decolorization effect was appeared in a mycelium-free decolorization system within pH 4.0–6.0 (Fig. 1c). However, when the pH value raised to 9.0, the decolorization rate dramatically increased to 93.6%. With mycelium, the decolorization rate increased when the pH varied from 4.0 to 6.0 and remained basically unchanged between pH 6.0 and 9.0. Thus, the initial pH 6 was selected to be an optimum value for MG decolorization with the maximum decolorization percentage (97.4%). When the pH is low, the mycelia are covered by a large amount of H^+, causing the mycelia to repel the positively charged cationic dye. However, higher pH conditions can convert the MG to a colorless but toxic derivative-leucomalachite green (LMG) instead of biodegradation (Chen et al., 2009). Appropriate pH value is vital to MG molecules binding to the surface of the organism. Previously, the optimal pH at which *Penicillium ochlochloron* degraded MG was 7 (Shedbalkar et al., 2008) and 6 for *Penicillium sp.* YW01 (Yang et al., 2011). Lv et al. (2013) observed that the proper pH for decolorization of MG by *Deinococcus radiodurans* R1 was from 6.0 to 8.0.

3.2 Metabolism analysis of MG degradation by *P. erygii*

The produced metabolites were identified by UPLC-Triple-TOF-MS/MS. The chromatogram of MG (control) had a conspicuous peak at 7.81 min and performed a mass of 329 *m/z*. Intermediate metabolites detected at 8.69, 7.45, 6.86, 6.13, and 2.80 min corresponded to the mass of 4-(dimethylamino)benzophenone (4-DMABP m/z 226), 4-(methylamino)benzophenone (4-MABP *m/z* 211), didemethyl MG (*m/z* 301), tridesmethyl MG (*m/z* 286), and 4-(dimethylamino)phenol (4-DMAP *m/z* 136). Similar to *Irpex lacteus* (Yang et al., 2016), P. *erygii* decomposed MG by two distinct mechanisms: N-demethylation and oxidative cleavage. Demethylation and hydroxylation are the different pathways catalyzed by *Cerrena* sp. (Yang et al., 2015) and *Phtotobacterium leiognathi* (Sutar et al., 2019). It was reported that the demethylating MG to form mono- and di-demethyl MG did not induce the decolorization of MG. Oxidative cleavage of the central C-C bonds can destroy the chromophore of MG, which is closely correlated with the decolorization of MG (Du et al., 2013; Mao et al., 2021).

The C-C bonds in the core region of MG might be broken by *P. erygii* to form 4-DMABP and 4-DMAP. Meanwhile, some MG is demethylated. Didemethyl MG, tridesmethyl MG, and 4-MABP detected during the reaction indicated that multiple demethylations by *P. erygii* occurred. The proposed metabolic pathways of MG by *P. erygii* are shown in Fig. 2. Despite the different formation pathways, metabolites 4-DMABP and 4-DMAP were detected in most MG biodegradation pathways (Yang et al., 2016; Xu et al., 2020). Some bacteria, fungi and enzymes may transform MG into higher toxic LMG (Jasin´ska et al., 2012; Shang et al., 2019; Song et al., 2020). The LMG was not detected in the intermediates in this study.

3.3 Toxicity study of MG degradation products

In preliminary experiments, we determined the toxicity of MG at different doses (1, 5, 20, 40, 100, and 200 μg/L) in zebrafish larvae and found that 100 and 200 μg/L of MG could cause significant liver damage. However, the zebrafish treated with 200 μg/L MG exhibited partial death during administration. Therefore, a 100 μg/L MG-induced toxicological model was selected in zebrafish larvae. With numerous advantages, the zebrafish is widely used as an appropriate model for evaluating drug toxicity and safety. Mao et al. (2021) discovered that 10% of zebrafish larvae exhibited evident tail deformation in 2 mg/L MG.

As shown in Fig. 3a and 3b, compared with the control group, zebrafish exposed to MG (100 μg/L) exhibited an opaque and dark liver with a reduced area (52.45 ± 3.49%, $p < 0.01$). In contrast, the degraded MG-treated group (100 μg/L, after 120 min of decolorization, > 99% decolorized) abated the liver damage of zebrafish by preventing atrophy. The same liver degeneration appearance in zebrafish was also found in other toxicological studies (Hill et al., 2012). Compared with the control group, the rates of liver transparency induced by MG and degraded MG were 85.42 ± 4.28% and 88.54 ± 5.11%, respectively. Statistically significant liver degeneration was observed between the control group and the other two groups. The liver degeneration was slightly alleviated in degraded MG-treated group; there was no statistical difference in the liver degeneration between the MG and degraded MG groups (Fig. 3c).

According to the results of H&E staining (Fig. 3d), in the control group, the liver tissue of zebrafish was normal, with intact and orderly arranged hepatocytes. However, in the liver tissue of the MG-exposed group, morphological changes, irregular arrangement and aggravation of vacuolation appeared. The degraded MG significantly attenuated the damage to zebrafish hepatocytes, suggesting a potential detoxification effect of *P. erygii*.

As a key immune organ for detoxification and material metabolism, liver can effectively reflect the effects of drugs (Thakkar et al., 2018). No developmental deformity of zebrafish was found in the control group. However, the malformation rate reached 10.89 ± 1.05% in the MG-treated group (100 μg/L), and it was reduced to 6.15 ± 0.89% after the degradation of *P. eryngii* (Fig. 4a). Compared to the control group, delayed yolk sac absorption was found in the MG-treated group (126.35 ± 4.59%) and the degraded MG-treated group (118.07 ± 3.82%) (Fig. 4b). The above findings suggested that the toxicity of MG to zebrafish was greatly reduced after degradation with *P. eryngii.* Zebrafish yolk is composed of 70% neutral lipid that is mainly metabolized in the liver (Jones et al., 2008). Thus, the yolk size can be seen as an indicator of zebrafish liver function, and the impairment of the liver could delay the yolk absorption.

3.4 Research on the DyP in *P. eryngii*

The DyP gene (1524 bp) was amplified from the genomic DNA of *P. eryngii* (Fig. 5a). The DyP gene encoded an open reading frame of 516 amino acids. To obtain the recombinant plasmid pCZN1-PE, the target segments were connected to pCZN1 vector and expressed in *E. coli* Rosetta expression cells. Intracellular proteins were obtained through cell disruption. After the DyP-PE protein was purified and analyzed, a single purified protein band of approximately 56.4 kDa was harvested (Fig. 5b). The protein

size was determined by comparing its migration in SDS-PAGE gels to that of the commercial molecular weight standards.

As shown in Fig. 5c, the decolorization efficiency of purified DyP-PE peroxidase for MG was tested at 30°C. A decrease in absorbance was monitored for up to 2 h. High efficiency of purified DyP-PE peroxidase was observed: at 0.05 mg/mL it could decolorize the MG up to 97.5%, 94.3%, and 90.2% at MG concentrations of 10, 20, and 30 mg/mL, respectively. This result indicates that DyP-PE peroxidase could effectively decolorize MG.

Previous studies have revealed that some oxidoreductases could degrade MG efficiently. The triphenylmethane reductase and cytochrome P450 oxygenase can catalyze the conversion of MG transform to LMG (Shang et al., 2019). MnP degrades MG by activating active enzyme with H_2O_2 (Yang et al., 2016). Developing new, simple and fast methods for the degradation of MG can be useful. The DyPs are famous for their potential applications in the degradation of various dyes (Hofrichter et al., 2010; Ren et al., 2022). DyPs were found in bacteria and fungi. Dhankhar et al. (2020) cloned and expressed the bacterial DyP from *Bacillus subtilis*, and the enzyme decolorized MG up to 73.63% within 30 min. A fungi DyP from *Ganoderma lucidum* and its crystal structures have been reported (Yoshida et al., 2011). We reported a newly discovered DyP-PE from *P. eryngii*.

4. Conclusion

In the present study, *P. eryngii* could efficiently decolorize MG under shaking conditions. Based on the identification of intermediates during the decolorization, a possible degradation pathway of MG by this strain has been proposed. N-demethylation and oxidation were used to breakdown MG, yielding five compounds. The toxicity tests of zebrafish indicated that this strain effectively detoxified MG. In addition, a 56.4 kDa DyP-PE from *P. eryngii* was cloned, overexpressed, and purified, and this enzyme exhibited good decolorizing properties of MG. This study demonstrates that *P. eryngii* has tremendous potential for treating MG effluent, and the DyP-PE in *P. eryngii* may contribute to the decolorization of MG.

Declarations

Author contributions *All authors contributed to the study conception and design. Material preparation, data collection and analysis were performed by* Guoying Lv, Yingyue Shen and Mei Wang. *The first draft of the manuscript was written by* Guoying Lv and Zuofa Zhang, *and all authors commented on previous versions of the manuscript. All authors read and approved the final manuscript.*

Funding The work was funded by the New Variety Breeding Project of Science Technology Department of Zhejiang Province (Grant number: 2021C02073).

Data availability The datasets used or analyzed during the current study are available from the corresponding author on reasonable request.

Ethical approval *Not applicable.*

Consent to participate *Not applicable.*

Consent for publication *Not applicable.*

Competing interests *The authors declare no competing interests.*

References

1. Adenan NH, Lim YY, Ting ASY (2022) Removal of triphenylmethane dyes by *Streptomyces bacillaris*: A study on decolorization, enzymatic reactions and toxicity of treated dye solutions. J Environ Manag 318:115520
2. Andersen WC, Casey CR, Nickel TJ, Yong SL, Turnipseed SB (2018) Dye residue analysis in raw and processed aquaculture products: matrix extension of AOAC INTERNATIONAL official method SM 2012.25. J AOAC Int 101:1927–1939
3. Arumugam TK, Krishnamoorthy P, Rajagopalan NR, Nanthini S, Vasudevan D (2019) Removal of malachite green from aqueous solutions using a modifed chitosan composite. Int J Biol Macromol 128:655–664
4. Chen CY, Kuo JT, Cheng CY, Huang YT, Ho IH, Chung YC (2009) Biological decolorization of dye solution containing malachite green by *Pandoraea pulmonicola* YC32 using a batch and continuous system. J Hazard Mater 172:1439–1445
5. Chaieb K, Altayb HN, Baothman OAS, Gomaa ABM, Nadeem MS, Kazmi I, Zamzami MA (2022) Molecular identifcation of indigenous halotolerant bacteria isolated from the red sea coast applied for biodegradation of synthetic dyes and assessment of degraded metabolite toxicity. Process Saf Environ 160:817–838
6. Daneshvar N, Ayazloo M, Khataee AR, Pourhassan M (2007) Biological decolorization of dye solution containing malachite green by microalgae *Cosmarium sp*. Bioresour Technol 98:1176–1182
7. Dhankhar P, Dalal V, Mahto JK, Gurjar BR, Tomar S, Sharma AK, Kumar P (2020) Characterization of dye-decolorizing peroxidase from *Bacillus subtilis*. Arch Biochem Biophys 693:108590
8. Du LN, Zhao M, Li G, Xu FC, Chen WH, Zhao YH (2013) Biodegradation of malachite green by *Micrococcus sp*. strain BD15: Biodegradation pathway and enzyme analysis. Int Biodeter Biodegr 78:108–116
9. Giri BS, Sonwani RK, Varjani S, Chaurasia D, Varadavenkatesan T, Chaturvedi P, Yadav S, Katiyar V, Singh RS, Pandey A (2022) Highly effcient bio-adsorption of malachite green using Chinese fan-palm biochar (*Livistona chinensis*). Chemosphere 287:132282
10. Gopinathan R, Kanhere J, Banerjee J (2015) Effect of malachite green toxicity on nontarget soil organisms. Chemosphere 120:637–644

11. Hadibarata T, Kristanti RA, Bilal M, Al-Mohaimeed AM, Chen TW, Lam MK (2022) Microbial degradation and transformation of benzo [a] pyrene by using a white-rot fungus *Pleurotus eryngii* F032. Chemosphere 307:136014
12. Hill A, Msens N, Steemans M, Xu JJ, Aleo MD (2012) Comparisons between in vitro whole cell imaging and in vivo zebrafish-based approaches for identifying potential human hepatotoxicants earlier in pharmaceutical development. Drug Metab Rev 44:127–140
13. Hofrichter M, Ullrich R, Pecyna MJ, Liers C, Lundell T (2010) New and classic families of secreted fungal heme peroxidases. Appl Microbiol Biotechnol 87(3):871–897
14. Jasin´ska A, Rózalska S, Bernat P, Paraszkiewicz K, Długon´ski J (2012) Malachite green decolorization by non-basidiomycete filamentous fungi of *Penicillium pinophilum* and *Myrothecium roridum*. Int Biodeterior Biodegrad 73:33–40
15. Jeon SJ, Lim SJ (2017) Purifcation and characterization of the laccase involved in dye decolorization by the white-rot fungus *Marasmius scorodonius*. J Microbiol Biotechnol 27:1120–1127
16. Jones KS, Alimov AP, Rilo HL, Jandacek RJ, Woolett LA, Penberthy WT (2008) A high throughput live transparent animal bioassay to identify non-toxic small molecules or genes that regulate vertebrate fat metabolism for obesity drug development. Nutr Metab (Lond) 5:23
17. Liu Y, Luo G, Ngo HH, Guo W, Zhang S (2020) Advances in thermostable laccase and its current application in lignin-frst biorefnery: A review. Bioresour Technol 298:122511
18. Lv GY, Cheng JH, Chen XY, Zhang ZF, Fan LF (2013) Biological decolorization of malachite green by *Deinococcus radiodurans* R1. Bioresour Technol 144:275–280
19. Mao G, Wang F, Wang J, Chen P, Zhang X, Zhang H, Wang Z, Song A (2021) A sustainable approach for degradation and detoxification of malachite green by an engineered polyphenol oxidase at high temperature. J Clean Prod 328:129437
20. Mohammed Al-Balawi, Zaheer A, Kosa Z SA (2023) Silver-platinum bimetallic nanoparticles as heterogeneous persulfate activator for the oxidation of malachite green. Arab J Chem 16(8):104863
21. Pandey D, Daverey A, Dutta K, Arunachalam K (2022) Bioremoval of toxic malachite green from water through simultaneous decolorization and degradation using laccase immobilized biochar. Chemosphere 297:134126
22. Rakhshaee R, Darvazeh J (2018) Studying role of air bubbles on suspension of hematite particles with three size ranges in plug flow reactor to improve dyes photo degradation compared to conventional packed bed photo reactors. J Hazard Mater 356:61–72
23. Ren J, Huo J, Wang Q, Liu Z, Li S, Wang S, Guo W, Li H (2022) Characteristics of immobilized dye-decolorizing peroxidase from *Bacillus amyloliquefaciens* and application to the bioremediation of dyeing effluent. Biochem Eng J 182:108430
24. Shang N, Ding M, Dai M, Si H, Li S, Zhao G (2019) Biodegradation of malachite green by an endophytic bacterium *Klebsiella aerogenes* S27 involving a novel oxidoreductase. Appl Microbiol Biotechnol 103(5):2141–2153

25. Shedbalkar U, Dhanve R, Jadhav J (2008) Biodegradation of triphenylmethane dye cotton blue by *Penicillium ochrochloron* MTCC 517. J Hazard Mater 15:472–479
26. Song J, Han G, Wang Y, Jiang X, Zhao D, Li M, Yang Z, Ma Q, Parales RE, Ruan Z (2020) Pathway and kinetics of malachite green biodegradation by *Pseudomonas veronii*. Sci Rep 10:1–11
27. Srivastav AK, Roy D (2018) Acute toxicity of malachite green (Triarylmethane dye) and pyceze (Bronopol) on carbohydrate metabolism in the freshwater fish *Heteropneustes fossilis* (Bloch). Int J Fish Aquat Stud 6(1):27–30
28. Sutar SS, Patil PJ, Tamboli AS, Patil DN, Apine OA, Jadhav JP (2019) Biodegradation and detoxification of malachite green by a newly isolated bioluminescent bacterium *Photobacterium leiognathi* strain MS under RSM optimized culture conditions. Biocatal Agric Biotechnol 20:101183
29. Thakkar S, Chen MJ, Fang H, Liu ZC, Roberts R, Tong WD (2018) The liver toxicity knowledge Base (LKTB) and drug-induced liver injury (DILI) classification for assessment of human liver injury. Expert Rev Gastroent 12:31–38
30. Ting ASY, Cheng CKW, Santiago KAA (2021) Decolourization of malachite green dye by endolichenic fungi from the lichen *Usnea sp.*: A novel study on their dye removal potential. J King Saud Univ Sci 33:101579
31. Vignesh A, Manigundan K, Santhoshkumar J, Shanmugasundaram T, Gopikrishnan V, Radhakrishnan M, Joseph J, Ayyasamy PM, Kumar GD, Meganathan R, Balagurunathan R (2020) Microbial degradation, spectral analysis and toxicological assessment of malachite green by *Streptomyces chrestomyceticus* S20. Bioproc Biosyst Eng 43:1457–1468
32. Xu KZ, Ma H, Wang YJ, Cai YJ, Liao XR, Guan ZB (2020) Extracellular expression of mutant CotA-laccase SF in *Escherichia coli* and its degradation of malachite green. Ecotox Environ Safe 193:110335
33. Yang J, Yang X, Lin Y, Ng TB, Lin J, Ye X (2015) Laccase-catalyzed decolorization of malachite green: performance optimization and degradation mechanism. PLoS ONE 10(5):e0127714
34. Yang X, Zheng J, Lu Y, Jia R (2016) Degradation and detoxification of the triphenylmethane dye malachite green catalyzed by crude manganese peroxidase from *Irpex lacteus* F17. Environ Sci Pollut Control Ser 23(10):9585–9597
35. Yang Y, Wang G, Wang B, Du L, Jia X, Zhao Y (2011) Decolorization of malachite green by a newly isolated *Penicillium* sp. YW 01 and optimization of decolorization parameters. Environ Eng Sci 28:555–562
36. Yoshida T, Tsuge H, Konno H, Hisabori T, Sugano Y (2011) The catalytic mechanism of dye-decolorizing peroxidase DyP may require the swimming movement of an aspartic acid residue. FEBS J 278(13):2387–2394
37. You X, Zhou R, Zhu YX, Bu DD, Cheng D (2022) Adsorption of dyes methyl violet and malachite green from aqueous solution on multi-step modified rice husk powder in single and binary systems: Characterization, adsorption behavior and physical interpretations. J Hazard Mater 430:128445

38. Zhang Z, Cai W, Song T, Fan L, Lv G (2021) Targeted identification of antioxidant compounds from *Sparassis latifolia* extracts and their antioxidant activities. J Food Process Pres 45(12):e16068
39. Zhou Y, Min Y, Qiao H, Huang Q, Wang E, Ma T (2015) Improved removal of malachite green from aqueous solution using chemically modified cellulose by anhydride. Int J Biol Macromol 74:271–277

Figures

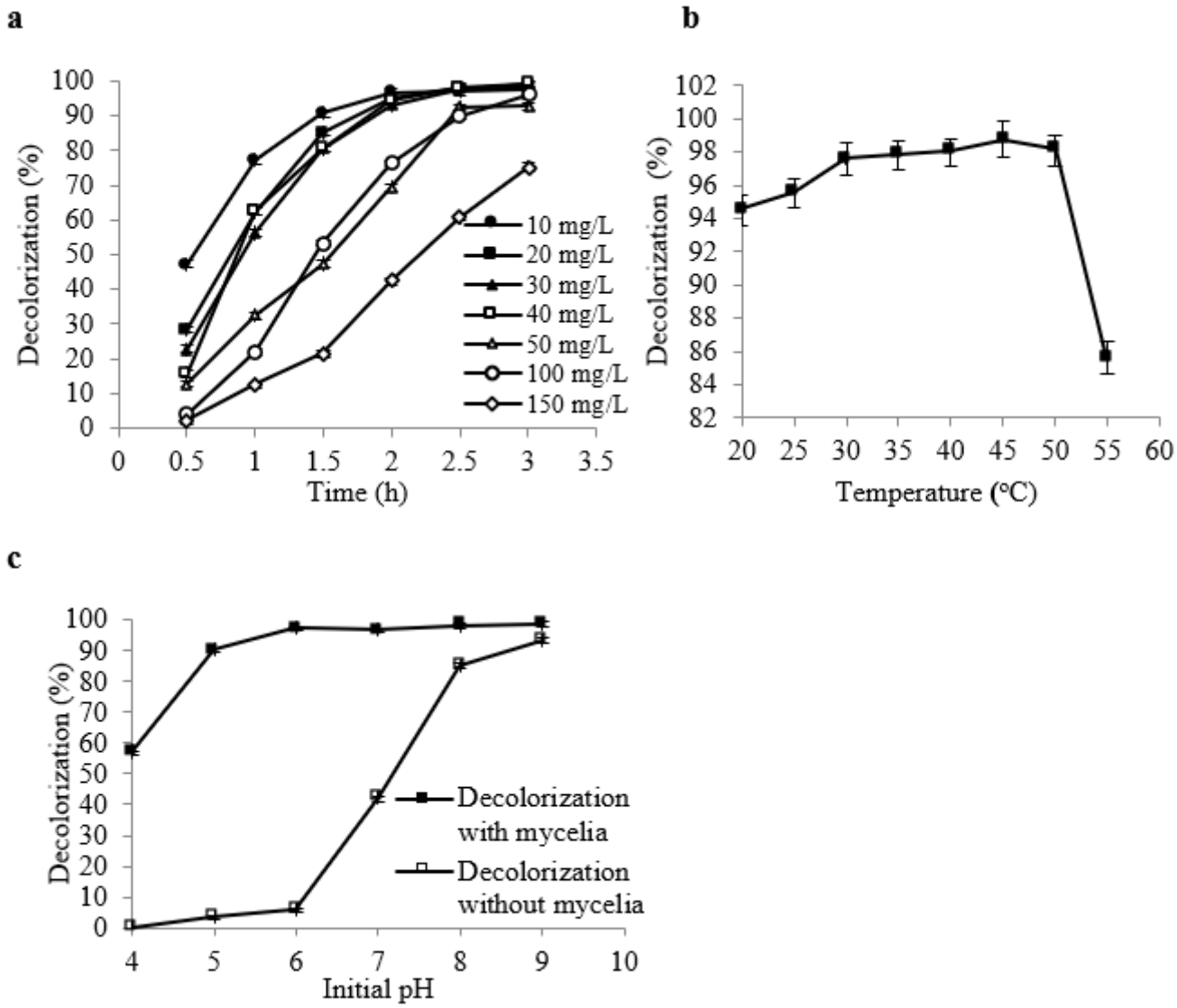

Figure 1

Decolorization of MG by *Pleurotus eryngii* (a) Effect of MG concentration and incubation time on the decolorization rate in the decolorization system, pH: 7.0, mycelium concentration: 10.0 g/L (wet weight), 25 ^{o}C, 50 r/min, (b) Effect of temperature on the decolorization rate of MG in the decolorization system, initial MG concentration: 20 mg/L, pH: 7.0, mycelium concentration: 10.0 g/L (wet weight), incubation time: 120 min, 50 r/min, (c) Effect of pH on the decolorization rate of MG in the decolorization system,

initial MG concentration: 20 mg/L, mycelium concentration: 10.0 g/L (wet weight), 30 ^{o}C, incubation time: 120 min, 50 r/min

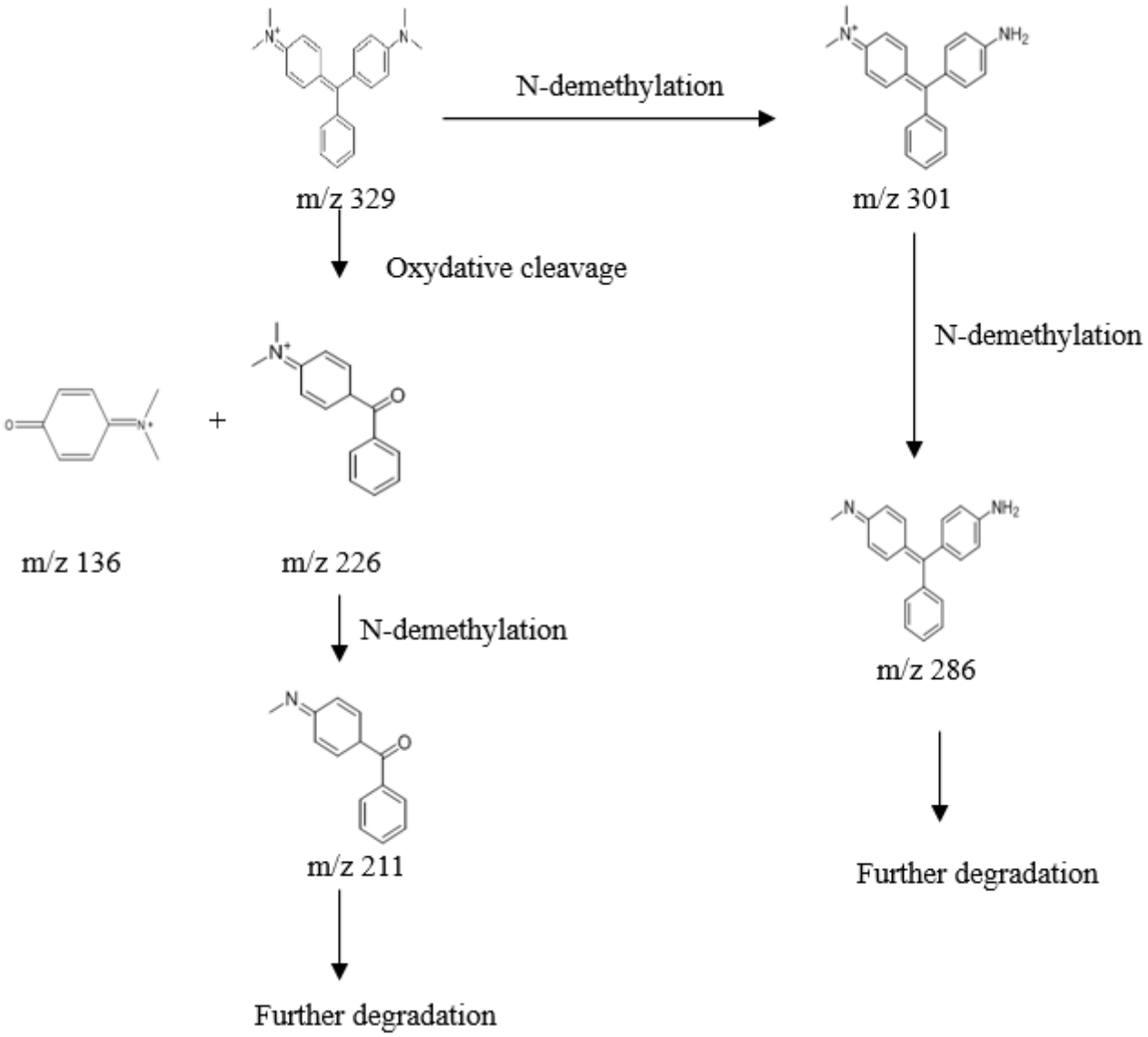

Figure 2

The proposed biodegradation pathways of MG by *P. eryngii* based on the results of UPLC-TOF-Triple-MSanalysis

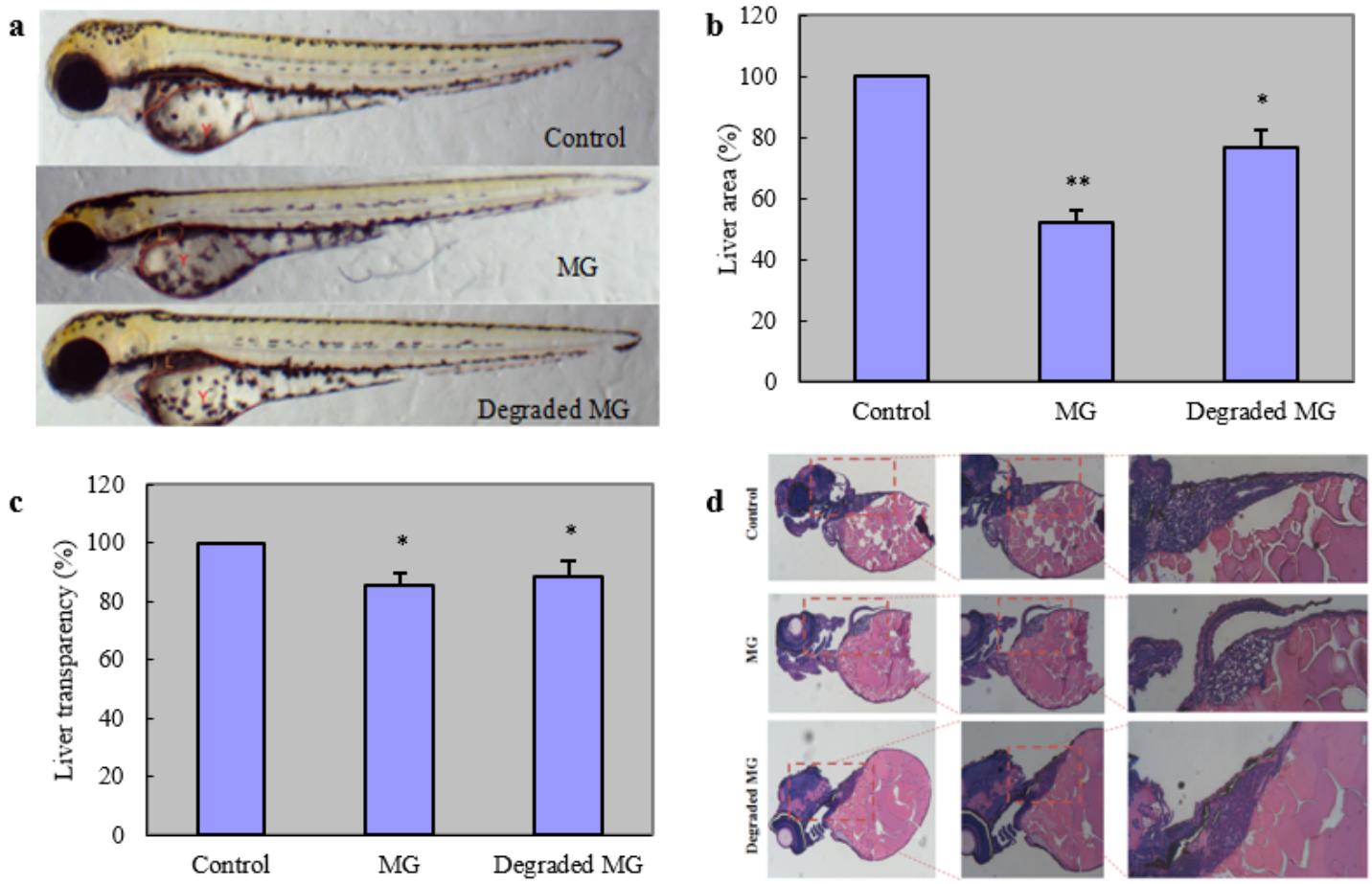

Figure 3

The effects of MG and degraded MG on liver of zebrafish larvae (a) liver color,(b) liver area, (c) liver transparency,(d) H&E staining. n=25, *P<0.05, **P<0.01 compared with the control group

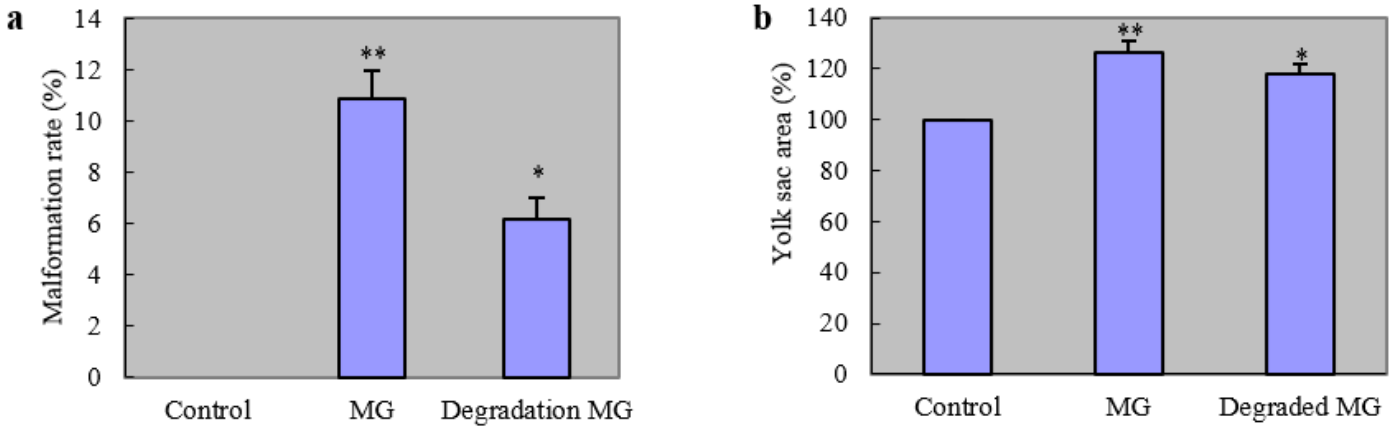

Figure 4

The effects of MG and degraded MG on malformation rate and yolk sac area of zebrafish larvae (a) malformation rate, (b) yolk sac area. n=25, *P<0.05, **P<0.01 compared with the control group

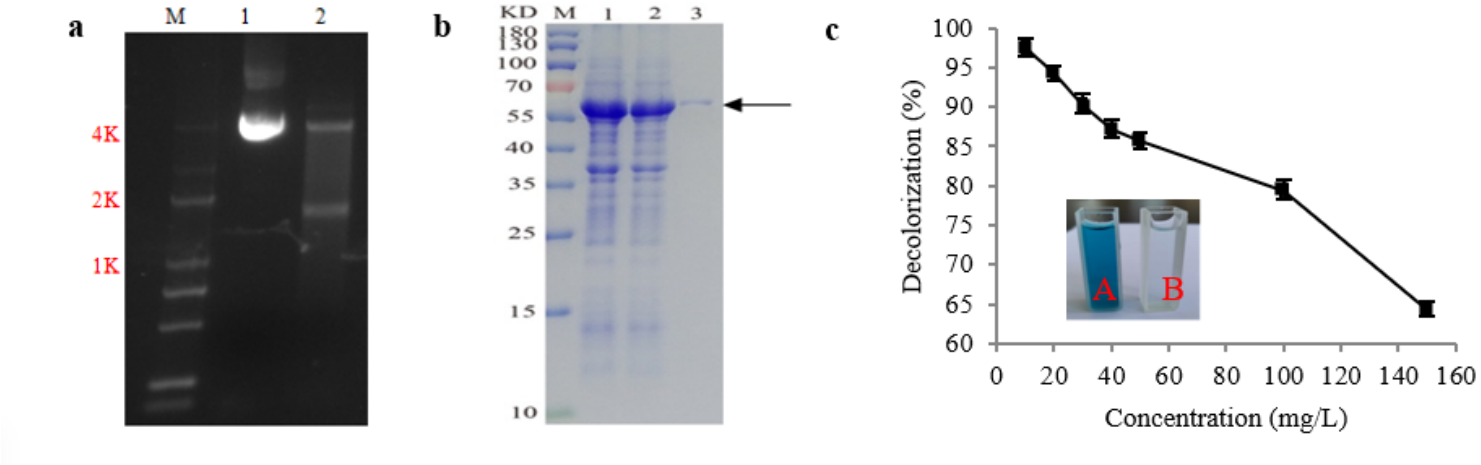

Figure 5

Purity analysis and capability to decolorize MG of DyP-PE (a) PCR test confirmation of DyP gene band of *P. eryngii*. Lane M: DNA maker, lane 2: plasmid, lane 3: plasmid digested with NdeI-XhoI, (b) SDS–PAGE band of purifed DyP-PE. Lane M: protein marker, lane 1 and 2: the cell lysate of overexpressed DyP-PE, lane 3: the purified DyP-PE, (c) MG decolorization catalyzed by the purified DyP-PE. A: control sample (20mg/L MG), B: degradation sample by the purified DyP-PE